AIP | Applied Physics Letters

Impact of carrier localization on radiative recombination times in semipolar (202¯1) plane InGaN/GaN quantum wells

R. Ivanov, S. Marcinkevičius, Y. Zhao, D. L. Becerra, S. Nakamura, S. P. DenBaars, and J. S. Speck

Citation: Applied Physics Letters **107**, 211109 (2015); doi: 10.1063/1.4936386
View online: http://dx.doi.org/10.1063/1.4936386
View Table of Contents: http://scitation.aip.org/content/aip/journal/apl/107/21?ver=pdfcov
Published by the AIP Publishing

Impact of carrier localization on radiative recombination times in semipolar $(20\bar{2}1)$ plane InGaN/GaN quantum wells

R. Ivanov,[1] S. Marcinkevičius,[1] Y. Zhao,[2] D. L. Becerra,[2] S. Nakamura,[2] S. P. DenBaars,[2] and J. S. Speck[2]
[1]*Department of Materials and Nano Physics, KTH Royal Institute of Technology, Electrum 229, 16440 Kista, Sweden*
[2]*Materials Department, University of California, Santa Barbara, California 93106, USA*

(Received 11 August 2015; accepted 12 November 2015; published online 25 November 2015)

Semipolar $(20\bar{2}1)$ plane $In_xGa_{1-x}N$ quantum wells (QWs) of varying alloy composition were studied by time-resolved photoluminescence. A large difference in effective radiative lifetimes, from sub-ns for $x = 0.11$ to ~30 ns for $x \approx 0.35$ was found. This effect is attributed to different properties of carrier localization. In low In content QWs, recombination at extended states with short recombination times is prevalent. In QWs with a high In content, the lifetimes are increased by localization of electrons and holes at separate sites. The zigzag shape of the QW interfaces and the resulting in-plane electric field are proposed as the cause for the separate electron and hole localization. © *2015 AIP Publishing LLC*. [http://dx.doi.org/10.1063/1.4936386]

Semipolar $(20\bar{2}1)$ plane $In_xGa_{1-x}N$/GaN quantum wells (QWs) have properties that make them an attractive alternative to commonly used polar QWs for light emitting device applications. First, they have a good In uptake allowing fabrication of devices emitting in the green and green-yellow spectral regions.[1–4] Second, the intrinsic electric field across the QWs caused by the difference of spontaneous and piezoelectric polarizations in the well and barrier layers is reduced by about six times.[5] This field reduction is expected to reduce the radiative recombination time and decrease the detrimental impact of the nonradiative and Auger recombination. So far, however, no thorough experimental investigations of carrier recombination that would confirm this theoretical prediction have been performed. The only study was limited to a QW structure emitting at ~530 nm.[6]

Apart from the intrinsic electric field, another effect, namely, the carrier localization, may affect the recombination times. This has been evidenced for ternary nitride QWs of different crystallographic orientations.[6–11] The localization may reduce or increase the nonradiative recombination rate via correlation or anticorrelation of the localization sites and defects. It may also affect the radiative rate by confining electrons and holes together into small localization regions or, on the contrary, separating them by localization at different sites.

In this work, we examine the recombination properties of $(20\bar{2}1)$ plane $In_xGa_{1-x}N$/GaN QWs with alloy composition varying in a wide range, $0.11 \leq x \leq 0.36$. Such an approach allows an exploration of general trends of carrier recombination in $(20\bar{2}1)$ plane QWs. The influence of the intrinsic electric field and the localization is assessed.

The studied QW structures were grown by metal organic chemical vapor deposition on low ($\sim 10^6\,cm^{-2}$) dislocation density bulk $(20\bar{2}1)$ plane GaN substrates provided by Mitsubishi Chemical Corporation. The structures consisted of a 1 μm undoped GaN template layer, a 3 nm thick $In_xGa_{1-x}N$ QW, and a 10 nm GaN cap layer. Indium content in the QWs of the studied structures was 0.11, 0.25, 0.31, 0.34, 0.35, and 0.36. Details of the growth procedure are described in Ref. 12. Photoluminescence (PL) spectra of all the samples had nearly Gaussian shape with room temperature peak wavelengths between 419 and 545 nm.[12] The PL peak linewidths were between 14 nm (100 meV) for $x = 0.11$ and 40 nm (170 meV) for $x \approx 0.35$.[12]

Carrier recombination was studied by means of time-resolved PL. For QWs with relatively short PL decay times, PL dynamics were measured using a frequency doubled pulsed Ti:sapphire laser (150 fs pulse duration, 390 nm central wavelength, 76 MHz pulse repetition frequency) and a spectrometer–streak camera system with 5 ps resolution. For measurements of long decay times, the pulse repetition frequency was reduced to 4 MHz with the help of a pulse picker based on an acousto-optic modulator. In the latter case, PL transients were recorded using band-pass filters and a time-correlated single photon counter with a resolution of 50 ps. The sample temperature was varied between 4 K and 300 K with the help of a closed cycle He cryostat. The 390 nm wavelength excitation generated carriers only in the QWs. The average pulse power was varied between 1.3 and 130 pJ, which, taking into account the excitation spot size and optical constants of GaN and InGaN, corresponds to photoexcited carrier densities between $1 \times 10^{10}\,cm^{-2}$ and $1 \times 10^{12}\,cm^{-2}$. Within this excitation range, the PL dynamics did not show any major dependence on the carrier density. Since focus of this paper is on the dependence of the radiative recombination on the QW alloy composition, the presented results are limited to the carrier density of $1 \times 10^{11}\,cm^{-2}$.

Figure 1 shows 4 K spectrally integrated PL transients for QWs with low, intermediate, and high In content. With an increased InN molar fraction, the PL decay, which, in general, is not single exponential, slows down.

Measurements with the streak camera system allow evaluating spectral changes occurring during the PL decay. In the experiments, no spectral shifts were observed. At low temperatures, when the radiative recombination is dominating, this indicates inhibited carrier transfer between localized sites; possibly, due to potential barriers between the

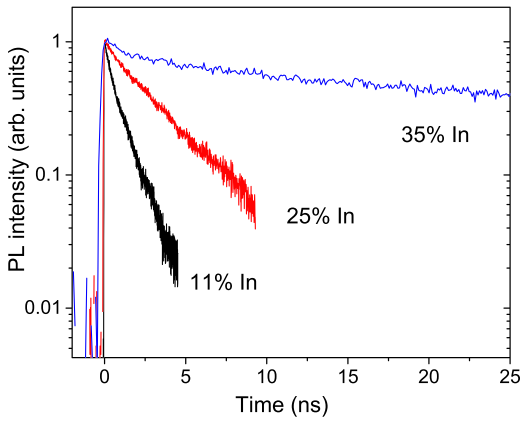

FIG. 1. Normalized 4 K PL transients for QWs with different InN molar fractions.

sites.[13,14] At high temperatures, at which the nonradiative recombination is prevailing (see below), the lack of the spectral shift shows that distribution of nonradiative recombination centers is spatially uniform, which is in line with the near-field PL data.[12]

PL decay times were evaluated by fitting transients with a model of a stretched exponential. The model describes the PL decay as $I_{PL}(t) \propto I_0 \exp[-(t/\tau_{eff})^{\beta}]$, where τ_{eff} is an effective decay time and β is the stretching parameter. In the model, the deviation from a single-exponential stems from the contribution of electrons and holes that are localized at separate potential minima and have varying transfer times into the same site for a rapid recombination.[15] More recent models[8,16] that emphasize a strong carrier localization in InGaN QWs have proposed a non-exponential PL decay shape that is supposed to be universal for all ternary nitride QWs. However, these models could not adequately fit all our data, probably due to the large contribution of the extended states, and, therefore, were not applied.

The fits for the 11% In QW PL transients measured at different temperatures provide β values in the interval from 0.8 to 0.9 indicating a weak deviation from the single exponential decay and a weak contribution of localization. This is consistent with the narrow PL linewidth and the small localization parameter value determined from the near-field PL scans.[12] For the larger In content QWs, the stretching factor obtained at different temperatures reduces to 0.3–0.5, showing an increased contribution of the localized carriers.

Effective radiative and nonradiative recombination times were determined from the transient peak and effective PL decay time values. In this approach[17,18] it is assumed that at 4 K the nonradiative recombination is negligible during the first few tens of ps until PL starts decaying, so that the transient peak value is not affected by the nonradiative recombination or trapping. This assumption is much weaker and should result in a smaller error than the supposition of the 100% internal quantum efficiency (IQE) often used in estimations of the recombination time. The 100% IQE implies a negligible nonradiative recombination during the whole time of the carrier recombination, which is often not correct.

The derived radiative and nonradiative lifetimes are effective values, representing corresponding averaged recombination processes.[19] The effective nonradiative lifetime describes the nonradiative recombination averaged over the probed QW volume. The effective radiative time convolutes the times of the rapid radiative recombination of carriers located at the same site and the slow recombination of spatially separated carriers, which may include different processes, as discussed below.

The temperature dependence of the PL decay time as well as the radiative and the nonradiative recombination times are gathered in Fig. 2. Both recombination times increase with the InN molar fraction. To understand the strong radiative lifetime dependence on the QW alloy composition, several effects were considered. First, the composition dependence of the intrinsic electric field was addressed. The field across the QWs and its influence on the electron and hole wave function overlap were calculated for QWs with flat interfaces using a one-dimensional Schrödinger and Poisson equation solver. The calculations show that the wave function overlap in the 36% In QW is only 10% smaller than in the 11% In QW (0.81 vs. 0.89). A larger wave function separation is prevented by the small QW width. Clearly, this small difference in the overlap cannot explain the large variation of the recombination times. Thus, the difference in the recombination times should have its origin in different properties of the carrier localization.

As mentioned above, the PL spectra broaden with an increased In content.[12] For the 11% QW, the near-field PL linewidth is determined by the homogeneous broadening and the random cation distribution in the alloy. For the higher In content QWs, the inhomogeneous broadening, induced by 1–10 nm scale band potential fluctuations, becomes important.

The carrier localization at the band potential fluctuations may affect the radiative lifetimes in several ways. If an

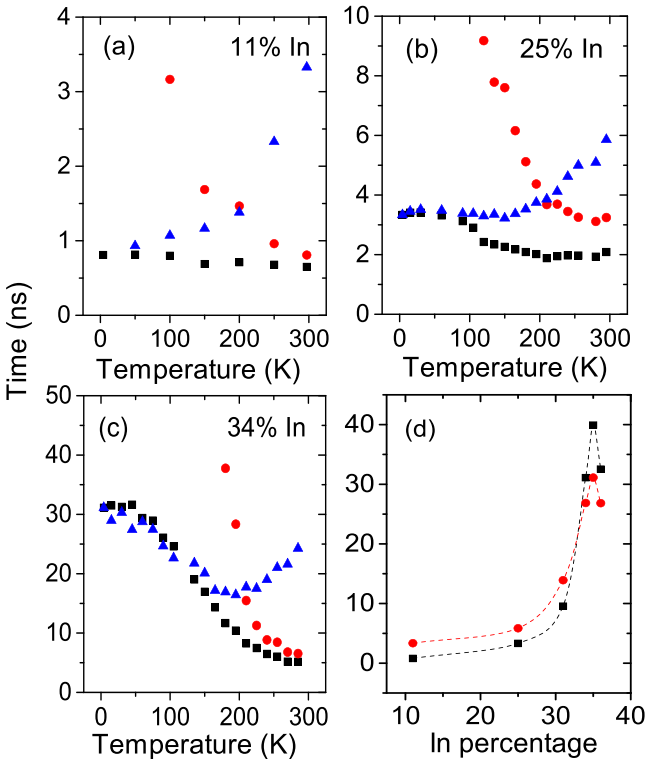

FIG. 2. Effective PL decay times (squares) and effective radiative (triangles) and nonradiative (dots) lifetimes for 11% (a), 25% (b), and 34% (c) In QWs. Part (d) shows 4 K (squares) and 300 K (dots) radiative time dependence on the InN molar fraction.

electron and a hole are localized in the same potential minimum of a size exceeding the exciton Bohr radius (~3 nm), and there is an in-plane electric field in the QW, the recombination time might be increased by the spatial carrier separation within the localization site. Alternatively, the radiative lifetime may be increased by the separate electron and hole localization at different sites.

A $(20\bar{2}1)$ plane QW with flat interfaces and a uniform alloy composition does not contain an in-plane component of the electric field. Spatial variations of the electric field might arise because of a partial strain relaxation or due to a non-planarity of the QW interfaces. Since the width of the studied QWs is well below the critical thickness even for $x = 0.36$,[20] no strain relaxation is expected. Hence, we will concentrate on the properties of the interfaces.

High-angle annular dark field (HADF) transmission electron microscopy imaging of a 3 nm thick $(20\bar{2}1)$ $In_{0.24}Ga_{0.76}N$ QW showed the presence of interfacial $(10\bar{1}0)$ and $(10\bar{1}\bar{1})$ nano-facets with a period of up to 4 nm.[21] With the help of the Comsol software package, we evaluated the influence that the interfacial faceting might have on the intrinsic electric field. In the simulations, interfaces with an ideal zigzag shape were considered (Fig. 3). Material parameters were taken from Ref. 22. Gauss equation was solved considering different discontinuities of the spontaneous polarization at the nanofacets. The polarization difference arises from the symmetry properties of the unit cell (e.g., there is no polarization discontinuity across an unstrained $(10\bar{1}0)$ nonpolar plane). The elastic strain of the QW was calculated using the generalized Hook's law for the $(20\bar{2}1)$ plane with an angle $\theta = 75°$ with respect to the c plane following Ref. 23. Charges induced by the piezoelectric effect were calculated for the real θ values of the nanofacets.

The simulations show that nanofaceting of the QW interfaces has a profound influence on the properties of the intrinsic field. The field is no longer perpendicular to the interfaces, but has a complex pattern with a non-negligible in-plane component. The magnitude of this component varies across the QW width with its amplitude reaching ~0.1 of the dominating perpendicular component. The in-plane field component oscillates with the undulation period (inset to Fig. 3). Its amplitude values at a distance of 1/4 of the well width from an equivalent flat interface are between 17 and 51 kV/cm for the wells with the In content of 0.11 and 0.36, respectively.

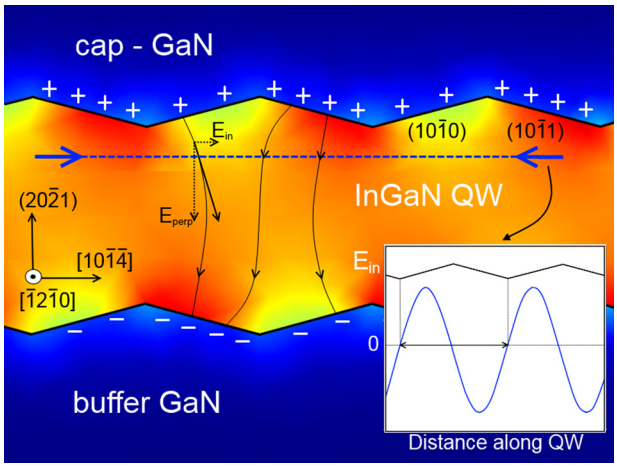

FIG. 3. Electric field distribution in a QW with zigzag nanofacet interfaces. The inset shows variation of the in-plane field component along the dashed line in the main plot.

The nanofacet planes and their period should not depend on the alloy composition. However, it is not known how strongly the nanofaceting is pronounced for different QWs. The HADF images are published only for $x = 0.24$.[21] They show that the faceting may be different for top and bottom QW interfaces and may be diffused, possibly, due to the intermixing. This prevents an exact estimation of the in-plane electric fields in real QWs. A qualitative evaluation of the importance of the non-planar interfaces for different alloy compositions can be made on the basis of the PL linewidth. The nanofaceting of the QW interfaces should contribute to the inhomogeneous broadening of the PL linewidth via well width variations. The PL linewidth for the 11% In QW has a negligible inhomogeneous broadening;[12] consequently, the nanofaceting for this QW should be minor. On the other hand, the inhomogeneous broadening in the high In content QWs is quite large. It is not clear which fraction of this broadening should be assigned to the well width variations and to the alloy composition fluctuations. Nevertheless, it is likely that the nanofaceting is more pronounced in the high In content QWs than in those with a low In percentage. This would make the difference in the in-plane field component for QWs of the different compositions even larger than the calculated values presented above.

The oscillating nature of the in-plane field with a small period of about 4 nm shows that this field cannot markedly affect the radiative lifetime of an electron hole pair localized at the same site. For a large site of ~10 nm, several periods of the oscillating field would average its influence on the wave functions. For smaller localization sites of 3–4 nm, the situation would resemble the case of the carrier confinement by the QW barriers in the growth direction, only with a much shallower confinement potential and a smaller electric field. To account for the 30-fold difference in the radiative times for the 11% In and ~35% In QWs, the wave function overlap should differ by about $\sqrt{30} \approx 5.5$ times. Clearly, the carrier separation by the in-plane field in the same localization site cannot account for such a difference.

Thus, the most likely mechanism leading to the long recombination times in the high In content QWs is the electron and hole localization at different sites. Several previous studies suggested that such localization is important;[9,10,16] however, the underlying mechanism was never discussed. The presence of the in-plane electric field could just be the reason of the electron and hole separation prior to their trapping to the localization sites. The in-plane field affects photoexcited carrier motion in the QW plane, where it is not restricted by the barriers. An order of magnitude estimation using a capture time from barriers into a QW of 300 fs (Ref. 24), an electron mobility in the QW of 300 $cm^2/(Vs)$ (Ref. 25) and an in-plane electric field of 10 kV/cm produces an electron transport distance of ~10 nm, which is similar to a likely distance between the localization sites.

An indirect argument for the relevance of the in-plane field can be found in the recombination data of nonpolar InGaN QWs with no interface faceting and a negligible in-

plane field. Despite that the localization potentials in *m*-plane QWs are deeper than in semipolar QWs,[13] the radiative recombination times are shorter, 0.5–2 ns.[18] Thus, the recombining electron hole pairs are either in the extended states or in the same localized states; i.e., no electron and hole separation into different localization sites occurs.

For an electron and a hole localized at separate sites, the recombination can either be spatially indirect or proceed via the electron transfer into the hole localization site. The transfer may take place via tunneling, thermionic emission, and by the combination of the two (Fowler-Nordheim tunneling). Using an analogy of the donor-acceptor pair recombination, it was proposed that the tunneling rate is determined by the distance r between the localized electron and the hole, and the exciton Bohr radius a as $1/\tau_{tun} \propto \exp(-r^2/a^2)$.[16] With increasing In content, the PL linewidth and the localization depth increase. Hence, one could expect that the density of the localization sites increases, and the distance between them decreases. According to the model, this would lead to shorter tunneling times in the high In content QWs, which is opposite to the experimental observations. Thus, the tunneling is not a likely process in our case. The inefficiency of the tunneling process allows setting the distance between the localization sites at least 3–5 nm.

On the other hand, the composition dependence of the radiative lifetimes correlates with the depth of the localization potentials hinting at the relevance of the thermal effects. The thermionic emission and thermally assisted tunneling rates depend on the localization energy (up to the mobility edge) ΔE as $\propto \exp[-\Delta E/(kT)]$.[26] Thus, a weakly localized electron has a higher probability to be thermally emitted from its localization sites and find a hole for a rapid recombination. Unfortunately, since several important parameters, such as the fraction of carriers that recombine from the extended and the localized states, and the energy separation between the localized states and the mobility edge are not known, a quantitative modelling of this process without adjustable parameters cannot be performed.

The relevance of separate electron and hole localization and thermal carrier excitation into less confined states is further demonstrated by the temperature dependence of the radiative recombination time (Figs. 2(a) and 2(c)) and the integrated PL intensity (Fig. 4). For the low In content QW, the PL intensity starts to decrease at ~60 K because of the nonradiative recombination. For the QWs with $x \approx 0.35$, the PL intensity in the interval from 4 K to 120 K increases by about 10%. This increase can be assigned to the increase of the radiative recombination rate because of the thermal carrier excitation to the sites with a weaker localization. With the shorter radiative lifetimes, the influence of the nonradiative recombination would become smaller, leading to the increased integrated PL intensity.

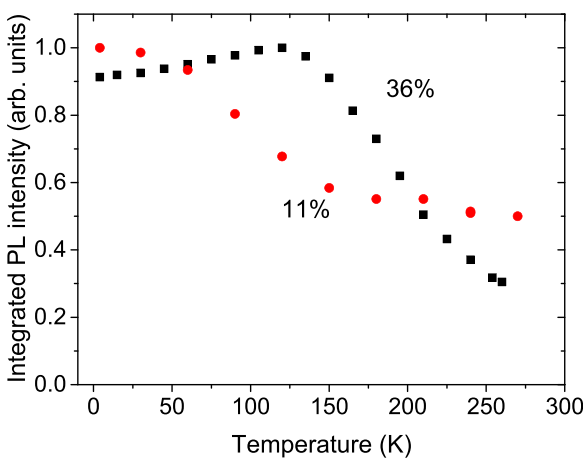

FIG. 4. Temperature dependence of normalized time- and spectrally integrated PL intensity for 11% and 36% In QWs.

The nonradiative recombination time increases with the In content as well. In homoepitaxial QW structures with a low dislocation density, point defects, impurities, and their complexes are the primary recombination centers.[27] The concentration of the common C and O impurities shows no major dependence on the growth conditions for semipolar planes.[28] The density of the point defects (Ga and N vacancies) is not expected to become lower with the increased In content. Thus, the increase of the nonradiative lifetime with the In percentage is likely to be determined by the carrier localization. Carriers localized at deep potential minima are less mobile and stay longer in the bands before being captured by the nonradiative recombination centers.

In summary, semipolar $(20\bar{2}1)$ plane InGaN QWs of varying alloy composition were studied by time-resolved PL. The experiments revealed a very large difference in effective radiative lifetimes, from sub-ns for $x = 0.11$ to about 30 ns for $x \approx 0.35$. This effect is attributed to the different properties of the carrier localization. In the low In content QWs, recombination in the extended states with short recombination times is prevailing. In the QWs with a high In percentage, the lifetimes are increased by localization of electrons and holes at different sites. The zigzag shape of the QW interfaces and the resulting in-plane electric field are proposed as the reason for this separate localization. Thus, one of the advantages of the semipolar QWs, namely, the increased rate of the radiative recombination due to the reduced vertical electric field, might be overshadowed by the effect of the separate electron and hole localization. Reduction of the band potential variations via improved growth technology seems to be critical in fulfilling the intrinsic potential of InGaN QWs with $(20\bar{2}1)$ crystallographic orientation for light emitting devices for the green spectral region.

The research at KTH was performed within the frame of Linnaeus Excellence Center for Advanced Optics and Photonics (ADOPT) and was financially supported by the Swedish Energy Agency (Contract No. 36652-1).

[1]Y. Enya, Y. Yoshizumi, T. Kyono, K. Akita, M. Ueno, M. Adachi, T. Sumitomo, S. Tokuyama, T. Ikegami, K. Katayama, and T. Nakamura, Appl. Phys. Express **2**, 082101 (2009).
[2]Y. Yoshizumi, M. Adachi, Y. Enya, T. Kyono, S. Tokuyama, T. Sumitomo, K. Akita, T. Ikegami, M. Ueno, K. Katayama, and T. Nakamura, Appl. Phys. Express **2**, 092101 (2009).
[3]R. B. Chung, Y. D. Lin, I. Koslow, N. Pfaff, H. Ohta, J. Ha, S. P. DenBaars, and S. Nakamura, Jpn. J. Appl. Phys. **49**, 070203 (2010).
[4]I. L. Koslow, C. McTaggart, F. Wu, S. Nakamura, J. S. Speck, and S. P. DenBaars, Appl. Phys. Express **7**, 031003 (2014).
[5]D. F. Feezell, J. S. Speck, S. P. DenBaars, and S. Nakamura, J. Disp. Technol. **9**, 190 (2013).
[6]M. Funato, A. Kaneta, Y. Kawakami, Y. Enya, K. Nishizuka, M. Ueno, and T. Nakamura, Appl. Phys. Express **3**, 021002 (2010).

[7]S. F. Chichibu, H. Marchand, M. S. Minsky, S. Keller, P. T. Fini, J. P. Ibbetson, S. B. Fleischer, J. S. Speck, J. E. Bowers, E. Hu, U. K. Mishra, S. P. DenBaars, T. Deguchi, T. Sota, and S. Nakamura, Appl. Phys. Lett. **74**, 1460 (1999).
[8]A. Morel, P. Lefebvre, S. Kalliakos, T. Taliercio, T. Bretagnon, and B. Gil, Phys. Rev. B **68**, 045331 (2003).
[9]V. Liuolia, S. Marcinkevičius, A. Pinos, R. Gaska, and M. S. Shur, Appl. Phys. Lett. **95**, 091910 (2009).
[10]T. Onuma, T. Koyama, A. Chakraborty, M. McLaurin, B. A. Haskell, P. T. Fini, S. Keller, S. P. DenBaars, J. S. Speck, S. Nakamura, U. K. Mishra, T. Sota, and S. F. Chichibu, J. Vac. Sci. Technol. B **25**, 1524 (2007).
[11]T. Langer, H.-G. Pietscher, F. A. Ketzer, H. Jönen, H. Bremers, U. Rossow, D. Menzel, and A. Hangleiter, Phys. Rev. B **90**, 205302 (2014).
[12]K. Gelžinytė, R. Ivanov, S. Marcinkevičius, Y. Zhao, S. P. DenBaars, S. Nakamura, and J. S. Speck, J. Appl. Phys. **117**, 023111 (2015).
[13]S. Marcinkevičius, K. M. Kelchner, S. Nakamura, S. P. DenBaars, and J. S. Speck, Appl. Phys. Lett. **102**, 101102 (2013).
[14]S. Marcinkevičius, K. Gelžinytė, Y. Zhao, S. Nakamura, S. P. DenBaars, and J. S. Speck, Appl. Phys. Lett. **105**, 111108 (2014).
[15]X. Chen, B. Henderson, and K. P. O'Donnell, Appl. Phys. Lett. **60**, 2672 (1992).
[16]C.-N. Brosseau, M. Perrin, C. Silva, and R. Leonelli, Phys. Rev. B **82**, 085305 (2010).
[17]E. Berkowicz, D. Gershoni, G. Bahir, E. Lakin, D. Shilo, E. Zolotoyabko, A. C. Abare, S. P. DenBaars, and L. A. Coldren, Phys. Rev. B **61**, 10994 (2000).
[18]S. Marcinkevičius, K. M. Kelchner, L. Y. Kuritzky, S. Nakamura, S. P. DenBaars, and J. S. Speck, Appl. Phys. Lett. **103**, 111107 (2013).
[19]S. F. Chichibu, T. Onuma, T. Aoyama, K. Nakajima, P. Ahmet, T. Chikyow, T. Sota, S. P. DenBaars, S. Nakamura, T. Kitamura, Y. Ishida, and H. Okumura, J. Vac. Sci. Technol. B **21**, 1856 (2003).
[20]D. L. Becerra, Y. Zhao, S. H. Oh, C. D. Pynn, K. Fujito, S. P. DenBaars, and S. Nakamura, Appl. Phys. Lett. **105**, 171106 (2014).
[21]Y. Zhao, F. Wu, T.-J. Yang, Y.-R. Wu, S. Nakamura, and J. S. Speck, Appl. Phys. Express **7**, 025503 (2014).
[22]P. Rinke, M. Winkelnkemper, A. Qteish, D. Bimberg, J. Neugebauer, and M. Scheffler, Phys. Rev. B **77**, 075202 (2008).
[23]A. E. Romanov, T. J. Baker, S. Nakamura, and J. S. Speck, J. Appl. Phys. **100**, 023522 (2006).
[24]Ü. Özgür and H. O. Everitt, Phys. Rev. B **67**, 155308 (2003).
[25]I.-L. Lu, Y.-R. Wu, J. M. Hinkley, and J. Singh, Proc. SPIE **7602**, 76021H (2010).
[26]H. Schneider and K. von Klitzing, Phys. Rev. B **38**, 6160 (1988).
[27]S. Marcinkevičius, Y. Zhao, S. Nakamura, S. P. DenBaars, and J. S. Speck, Appl. Phys. Lett. **104**, 111113 (2014).
[28]S. C. Cruz, S. Keller, T. E. Mates, U. K. Mishra, and S. P. DenBaars, J. Cryst. Growth **311**, 3817 (2009).